Available online at www.sciencedirect.com
SCIENCE DIRECT®
Bioorganic & Medicinal Chemistry Letters 15 (2005) 271–276
Bioorganic & Medicinal Chemistry Letters

Structure based approach to the design of bicyclic-1*H*-isoindole-1,3(2*H*)-dione based androgen receptor antagonists

Mark E. Salvati,[a,*] Aaron Balog,[a] Weifang Shan,[a] Donna D. Wei,[a] Dacia Pickering,[a] Ricardo M. Attar,[b] Jieping Geng,[b] Cheryl A. Rizzo,[b] Marco M. Gottardis,[b] Roberto Weinmann,[b] Stanley R. Krystek,[c] John Sack,[c] Yongmi An[c] and Kevin Kish[c]

[a]*Department of Oncology Chemistry, Bristol-Myers Squibb Pharmaceutical Research Institute, PO Box 4000, Princeton, NJ 08543-4000, USA*
[b]*Department of Discovery Biology, Bristol-Myers Squibb Pharmaceutical Research Institute, PO Box 4000, Princeton, NJ 08543-4000, USA*
[c]*Department of Macromolecular Structure, Bristol-Myers Squibb Pharmaceutical Research Institute, PO Box 4000, Princeton, NJ 08543-4000, USA*

Received 13 August 2004; revised 20 October 2004; accepted 30 October 2004
Available online 21 November 2004

Abstract—A novel series of isoindoledione based compounds were identified as potent antagonists of the androgen receptor (AR). Co-crystallization of members of this family of inhibitors was successfully accomplished with the T877A AR LBD. A working model of how this class of compounds functions to antagonize the AR was created. Based on this model, it was proposed that expanding the bicyclic portion of the molecule should result in analogs which function as effective antagonists against a variety of AR isoforms. In contrast to what was predicted by the model, SAR around this new series was dictated by the aniline portion rather than the bicyclic portion of the molecule.

Carcinoma of the prostate (CaP) is the second leading cause of cancer related death in men with an estimated 182,000 new cases diagnosed and 40,000 deaths each year in the United States.[1] For the past 50 years, androgen ablation via castration has been the most effective therapy for the treatment of advanced CaP in the clinic. A more recent treatment alternative, complete androgen blockade (CAB) is accomplished by treatment with an androgen receptor antagonist in combination with chemical castration via a luteinizing hormone releasing hormone agonist.[2] Although this approach initially shows a 80–90% response rate,[3] when treatment is continued for 1–2 years, approximately 50% of patients progress to fatal androgen independent disease.[4] Clearly, there is an unmet medical need for the treatment of advanced CaP. For this reason, we are interested in identifying novel small-molecule antagonists of the AR that are more effective than the current therapies.

As previously described, we have discovered a novel series of bicyclic 1*H*-isoindole-1,3(2*H*)-diones that function as potent AR antagonists.[5] Preliminary structure–activity data, comprising AR binding and functional response in whole cell assays, indicated that both intrinsic receptor affinity and agonist/antagonist profiles could be modulated. Our earlier empirical methods generated clear SAR for the wild type AR, but failed to show a correlation across a series of AR isoforms. Therefore, we attempted to identify clear SAR trends for this series by capitalizing on AR structural information that was experimentally derived in our laboratories.[6] This report describes our structure-based approach to the design of potent, broad spectrum AR antagonists, and provides a retrospective analysis of our findings.

As shown in Table 1, screening revealed that certain members of this series (**3**) gave an in vitro profile similar

Keywords: Androgen receptor; Antagonists; Crystal structure; Prostate cancer.
* Corresponding author. Tel.: +1 609 252 4204; fax: +1 609 252 7410; e-mail: mark.salvati@bms.com

0960-894X/$ - see front matter © 2004 Elsevier Ltd. All rights reserved.
doi:10.1016/j.bmcl.2004.10.085

Table 1. Initial AR antagonist leads

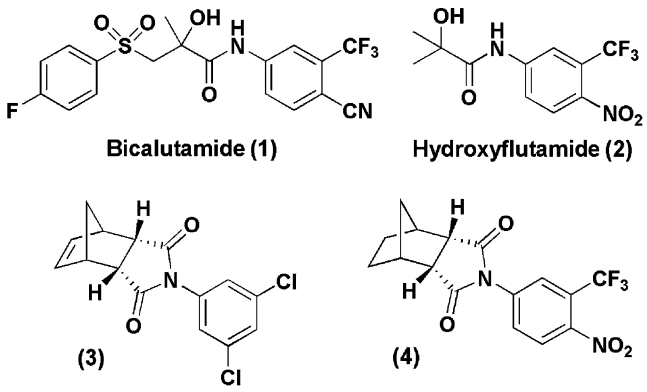

Compd no	MDA-453 K_i, nM[a]	MDA-453 IC_{50}, nM[b]	LNCaP K_i, nM[a]	LNCaP IC_{50}, nM[b]	PCa2b IC_{50}, nM[c]
1	64	173	35	400	725
2	43	26	2	Ag[d]	Ag[d]
3	158	307	6	41	180
4	5	12	2	Ag	Ag

[a] Binding determined through direct displacement with [^{3}H]-DHT in the MDA-453 cell line (K_i) or in the LNCaP cell line.[8]
[b] Functional antagonist activity determined through a transiently transfected reporter assay system utilizing a secreted alkaline phosphatase (SEAP) reporter construct and a PSA AR promoter domain.[8]
[c] Inhibition of cell proliferation determined by [^{3}H]-thymidine incorporation over a 72 h growth period.[8]
[d] Ag: Compounds were run through the assays described in footnotes 'b' and 'c' in the presence or absence of the AR agonist ligand DHT. In the absence of DHT, these compounds were able to activate the AR in the transcription assays or promote the growth of the PCa2b cell line, thus behaving as agonists (Ag) ligands for the AR. In the presence of DHT these compounds showed minimal to no measurable antagonist activity.

to the clinical antiandrogen bicalutamide[3] (**1**), having an antagonist profile (IC_{50}) toward the mutant T877A AR in the LNCaP[7] cell line and inhibiting the androgen dependent growth of the human prostate cancer cell line MDA-MB-PCa2b, which contains an AR with mutations at both L701H and T877A.[5,8] In contrast, other members of the series (**4**) gave a profile similar to the active metabolite of the clinical antiandrogen flutamide[3] (**2**), having an agonist profile toward the LNCaP and MDA-MB-PCa2b cell lines. The goal of our initial SAR studies was to optimize the antagonist profile of this series across an array of AR isoforms by probing the effects of substituents around the aniline and bicyclic portion of the molecule through parallel synthesis approaches. Initial studies suggested that the aniline portion of the molecule dictated binding and functional activity, leaving the role of the bicyclic portion of the molecule unclear. As modifying the bicyclic portion of the molecule in a parallel synthesis approach proved to be challenging, we set out to utilize approaches of rational drug design to approach the question of how to impart an antagonist profile across a series of AR isoforms.

To gain insight into the binding of our lead series to the AR at the molecular level, we set out to generate a co-crystal structure of our lead series with the AR ligand binding domain (LBD). Based on our previous success in obtaining co-crystals of the WT and T877A AR LBD bound to the natural agonist ligand DHT[6] and the knowledge that several of our ligands behaved as agonists toward the MT AR isoforms, we decided to pursue co-crystallization with the T877A AR LBD as our primary strategy. Figure 1A shows a rendering of the co-crystal of the T877A AR LBD with compound **5** (Table 2) resolved to 1.8 Å.[9] Several key structural features became evident when comparing this structure to the available structure of DHT bound to the T877A AR LBD shown in Figure 1B. Although the backbone structure of the proteins bound with either DHT or compound **5** generate a superimposable agonist conformation, the two ligands clearly bound in a different fashion. It is important to note that this structure is the first clear evidence that small molecule antiandrogens, which demonstrate an agonist profile in the LNCaP cell line, generate an agonist conformation with the A877 AR LBD. The 4-nitro group on the naphthyl system appears to take the place of the C-3 carbonyl of DHT, making similar contacts with both arginine 752 (R752) and glutamine 711 (Q711). In the case of DHT, a water molecule is also bridged from the C-3 carbonyl group to R752 and Q711. No such water molecule is found when **5** binds into the ligand binding pocket. As can be seen, phenylalanine 764 (F764) forms an edge face interaction with the first aromatic ring of the naphthyl system of **5**, in a fashion similar to that seen with the A ring of DHT. Unlike DHT, the second aromatic ring of the naphthyl system of **5** occupies a hydrophobic pocket not occupied when DHT is bound. With DHT, the D-ring region participates in a bifurcated H-bond from the C-17 hydroxyl to asparagine 705 (N705), and in the case of the WT AR, threonine 877 (T877). The lipophilic bicyclic portion of **5** occupies the same position in the ligand binding pocket of AR as the C and D rings of DHT, but offers no substituents to form hydrogen bonds with available sites in this region of the protein.

The most interesting piece of information gleaned from the structure of the T877A AR LBD was the fact that the imide portion of the molecule generates no

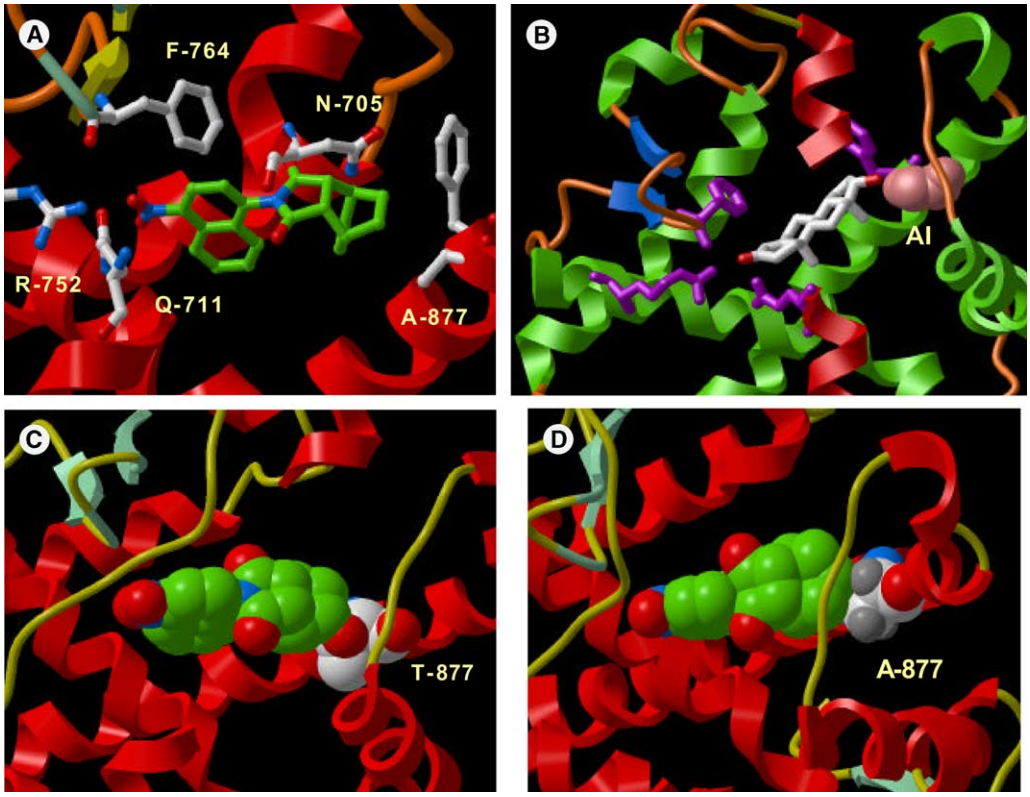

Figure 1. (A) Crystal structure of the T877A AR LBD and compound **5** at 1.8 Å. View of T877A AR LBD binding site with a portion of the backbone ribbon (red) removed for clarity. Key side chains are displayed and colored by atom type (C white, N blue, O red). Compound **5** is shown in stick colored by atom type (C green, N blue, O red). (B) Crystal structure of the T877A AR LBD and DHT at 1.8 Å. View of T877A AR LBD binding site with a portion of the backbone ribbon (red) removed for clarity. Key side chains are displayed in purple. Alanine 877 is show in space filling in pink. DHT is shown in stick colored by atom type (C green, N blue, O red). (C) Molecular overlay of WT AR LDB co-crystallized with DHT and mutant AR T877A with compound **5** displayed in space-filling colored by atom type (C green, N blue, O red). T877 of WT AR LBD is displayed in space filling (colored C white, N blue, O red). (D) Molecular overlay of the T877 AR LDB co-crystallized with compound **5** in which compound **5** is replaced by compound **7** displayed in space-filling colored by atom type (C green, N blue, O red). A877 of MT AR LBD is displayed in space filling (colored C white, N blue, O red, H gray).

Table 2. SAR of bicyclo[3.2.2]nonane analogs

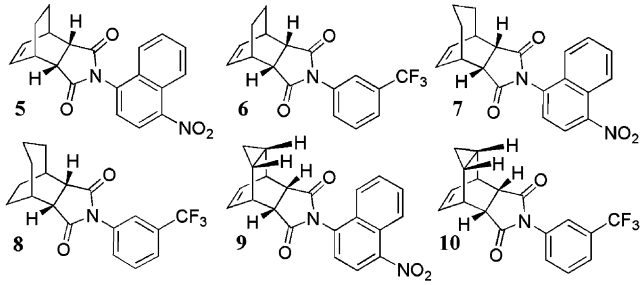

Compd no	MDA-453 K_i, nM[a]	MDA-453 IC_{50}, nM[b]	LNCaP K_i, nM[a]	LNCaP IC_{50}, nM[b]	PCa2b IC_{50}, nM[a]
5	19	224	0.5	Ag[d]	Ag[d]
6	100	196	19	66	0.4
7	9	49	9	Ag[d]	Ag[d]
8	2810	658	20	23	179
9	3	786	NT[e]	Ag[d]	Ag[d]
10	3200	1700	9	30	148

[a–d] See footnotes of Table 1.
[e] NT: Not tested.

significant interactions with any residues in the LBD. Since most of the known small molecule AR antagonists contain an aryl amide functionality isosteric with the imide portion of **5** (see Table 1, compounds **1** and **2**),

we assumed that the carbonyl or the amide nitrogen made some critical H-bond interaction within the LBD that contributed to the binding affinity. No residues capable of forming a hydrogen bond or Van der Waals interactions could be found within 5 Å of either the carbonyls or the nitrogen atom of the imide system. At this point it is our assumption that the imide portion of the molecule serves only to constrain the bicyclic and aniline portions of the molecule into a geometry that optimizes binding. For **5**, with the exception of interactions at the aniline portion of the molecule, tight binding to the AR ligand binding pocket is driven by aromatic and hydrophobic interactions with residues of the AR ligand binding pocket.

With the structure of **5** bound in the T877A AR LBD in hand, we next sought to understand why a simple transformation from a threonine to an alanine at position 877 of the AR LBD resulted in the reversal of **5** from a functional antagonist toward the WT AR to a functional agonist toward the MT AR. To this end, we superimposed the co-crystal structure of the WT AR LBD with DHT bound over the co-crystal structure of the T877A AR LBD with **5** bound (Fig. 1C).[10] No significant differences were noted in the backbone structure of the two proteins despite the single point mutation and the dramatically different ligands bound to the active sites. Space filling rendering of **5** and the threonine residue at position 877 clearly illustrates that the bicyclic portion (green) of **5** will clash with the polar threonine (white) residue in the WT AR LBD. This situation does not occur in the T877A AR LBD due to the smaller size and lipophilic nature of the alanine residue. We believe that the clash between the bicyclic system and the threonine residue leads to movement in helix-3 and/or helix-10/11, which ultimately leads to displacement of helix-12 and the generation of an antagonist-like conformation with the WT AR. The above hypothesis seems to give a plausible explanation for why compounds which demonstrate antagonist activity in the WT AR, can behave as agonists with the MT AR found in the LNCap and PCa2b cell lines, since the mutations found in each receptor creates additional space in the binding pocket around the portion which accommodates the D-ring of DHT. This hypothesis, however, does not explain the previously described SAR for this series, which demonstrates that the aniline portion of the molecule, which makes no direct interactions with the mutations found in either receptor, dominates the functional activity of this series of antagonists. The discrepancy between the structural information and the observed SAR may reflect the fact that our interpretations are based on structural information on the AR LBD in an agonist rather than an antagonist conformation.

In order to validate the above proposed model for antagonism of the AR, we set out to design a new series of agents that would inhibit both the WT as well as MT AR isoforms. Based on the model shown in Figure 1C, we theorized that expanding the size of the bicyclic system should result in a similar steric clash with the alanine residue in the T877A AR, resulting in compounds which will retain an antagonist profile against either the WT or MT AR isoforms. Figure 1D shows a docking model of the bicyclo[3.2.2]nonane analog **7** (Table 2) bound to the T877A AR LBD. Space filling rendering of **7** (green) and the alanine residue (white) at position 877 suggests that the bicyclic portion of **7** will clash with the alanine residue in a fashion similar to that seen in Figure 1B, possibly leading to an antagonist conformation.

Based on the binding models and structures described above, we set forth making a new series of AR antagonists having an expanded ring size beyond the bicyclo-[2.2.1]heptane and bicyclo[2.2.2]octane systems previously explored. Modeling suggested that expanding the ring size by just one carbon unit, to generate a bicyclo[3.2.2]nonane system, would be sufficient to result in a steric clash with A877 of the MT AR while not being too large to fit into the WT AR binding pocket. To this end, we explored the SAR around a series of bicyclo[3.2.2]nonane and cyclopropyl-bicyclo[2.2.2]octane analogs. Table 2 gives a brief overview of the SAR obtained around this series of analogs, the synthesis of which has been described in detail previously.[5,11] A clear trend that was noted from this series was that functional activity against the MT AR isoforms found in the LNCaP and PCa2b cell lines was dictated by the aniline portion of the molecule, not by the bicyclic portion. As can be seen, when the 4-nitronaphthyl group is employed, an agonist profile is seen for the bicyclo-[2.2.2]octane analog **5** and the larger bicyclo[3.2.2]nonane analogs **7** and **9**. In contrast, when the 3-trifluoromethylaniline is used, a full antagonist profile is seen for all analogs (compare **6**, **8** and **10**) with little change in binding to the T877A AR or functional activity with either MT AR cellular assays. The effect of increasing the size of the bicyclic ring was much more dramatic with the WT AR. When the 4-nitronaphthyl group was employed, as the ring size increased, the binding, and to some extent the functional activity, increased. In sharp contrast, when 3-trifluoromethylaniline is used, a significant loss of both binding and functional activity is seen as the ring size increases. Both of these examples suggest that it is the aniline portion, which dictates both the binding and functional activity within this series of compounds. This trend is not consistent with the model we set out to validate but is consistent with earlier SAR seen for this series of AR antagonists.

In addition to the simple bicyclo[3.2.2]nonane analogs described in Table 2, a diverse array of bicyclo[2.2.2]-octane analogs, with substitution around the bicyclic ring, was prepared (Table 3).[12] These and other related compounds[5] were developed in an effort to validate our proposed model for antagonism of the AR. In general, we could not establish any clear trends for substitution around the bicyclic system and the production of an antagonist profile across a series of AR isoforms. In fact, varying the substitution around the bicyclic system caused a more diverse pattern of activity, with compounds now demonstrating different profiles in the different MT isoforms (see compound **12**). For the WT AR found in the MDA-453 cell line, increasing the bulk around the bicyclic ring in general lead to a decrease in

Table 3. SAR of bicyclo[3.2.2]nonane analogs

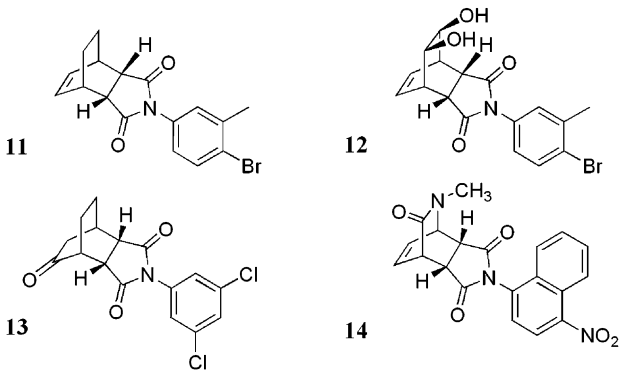

Compd no	MDA-453 K_i, nM[a]	MDA-453 IC_{50}, nM[b]	LNCaP K_i, nM[a]	LNCaP IC_{50}, nM[b]	PCa2b IC_{50}, nM[c]
11	171	68	0.01	Ag[d]	Ag[d]
12	432	5240	33	59	Ag[d]
13	83	150	28	Ag[d]	Ag[d]
14	>5000	4030	115	631	8460

[a–d]See footnotes of Table 1.

binding and functional activity (see compounds **12** and **14**). Some modifications were noted that lead to an increase in binding to the WT AR, however, this often did not translate into an increase in functional activity (compare compounds **11** and **13**).

In summary, we have developed and characterized a novel series of bicyclic-1*H*-isoindole-1,3(2*H*)-dione based androgen receptor antagonists. These compounds demonstrate potent binding to and functional antagonist activity against the WT AR. In addition, members of this family demonstrate potent binding and functional antagonist activity toward the T877A AR found in the LNCaP human prostate cancer cell line, as well as potent growth inhibitory activity against the MDA-MB-PCa2b human prostate cancer cell line, which contains a doubly mutated L701H and T877A AR. Co-crystallization of members of this family of inhibitors was successfully accomplished with the T877A AR LBD. This structural information was utilized to build a working model of how compounds in this class function to antagonize the AR. Based on this model it was predicted that a new series of analogs in which the bicyclic portion of the molecule was expanded should function as antagonists to the WT as well as MT AR isoforms. In contrast to what was predicted by the model, SAR suggests that the aniline portion of this family of inhibitors dictates both the binding and functional activity across all isoforms of the AR that were explored. While we were not able to completely reconcile our limited experimental results with the structural based hypothesis proposed, this account represents our first efforts toward building a model for understanding, at a molecular level, the attributes that lead to an effective AR antagonist.

References and notes

1. Jemal, A.; Thomas, H.; Murray, T.; Thun, M. *CA Cancer J. Clin.* **2002**, *52*, 23.
2. (a) Gao, K. L. *Drugs* **1991**, *43*, 254; (b) Motta, M.; Serio, M. *Hormonal Therapy of Prostatic Diseases: Basic and Clinical Aspects*; Medicom Europe: Amsterdam, 1998; (c) Crawford, E. D.; DeAntonio, E. P.; Labrie, F.; Schroder, F. H.; Geller, J. *J. Clin. Endocrinol. Metab.* **1995**, *80*, 1062.
3. (a) Blackledge, G. *Cancer* **1993**, 3830; (b) Maucher, A.; von Angerer, E. *J. Cancer Res. Clin. Oncol.* **1993**, *119*, 669; (c) Sufrin, G.; Coffey, D. S. *Invest. Urol.* **1976**, *13*, 429; (d) Narayana, A. S.; Loening, S. A.; Culp, D. A. *Br. J. Urol.* **1981**, *53*, 152.
4. (a) Huggins, C.; Stevens, R.; Hodges, C. V. *Arch. Surg.* **1947**, *43*, 209; (b) Westin, P.; Stattin, P.; Damber, J.-E.; Bergh, A. *Am. J. Pathol.* **1995**, *146*, 1368.
5. (a) Balog, A.; Salvati, M. E.; Shan, W.; Mathur, A.; Leith, L. W.; Wei, D. D.; Attar, R. M.; Geng, J.; Rizzo, C. A.; Wang, C.; Krystek, S. R.; Tokarski, J. S.; Hunt, J. T.; Gottardis, M.; Weinmann, R. *Bioorg. Med. Chem. Lett.* **2004**, *14*, 6107; (b) Salvati, M. E.; Balog, A.; Wei, D. D.; Pickering, D.; Attar, R. M.; Geng, J.; Rizzo, C. A.; Hunt, J. T.; Gottardis, M. M.; Weinmann, R.; Martinez, R. *Bioorg. Med. Chem. Lett.* **2005**, *15*, in press, doi:10.1016/j.bmcl.2004.10.051.
6. The structure of the T877A AR LBD complexed with **5** was resolved as described in: Sack, J. S.; Kish, K. F.; Wang, C.; Attar, R. M.; Kiefer, S. E.; An, Y.; Wu, G. Y.; Scheffler, J. E.; Salvati, M. E.; Krystek, S. R., Jr.; Weinmann, R.; Einspahr, H. M. *Proc. Natl. Acad. Sci. U.S.A.* **2001**, *98*, 4904. Coordinates for the above structure have been deposited into the Protein Data Bank with the code 1XNN.
7. Veldscholte, J.; Berrevoets, C. A.; Ris-Stalpers, C.; Kuiper, G. G. J. M.; Jenster, G.; Trapman, J.; Brinkman, A. O.; Mulder, E. *J. Steroid Biochem. Mol. Biol.* **1992**, *41*, 665.
8. (a) Navone, N. M.; Olive, M.; Ozen, M.; Davis, R.; Troncoso, P.; Tu, S.-M.; Johnston, D.; Pollack, A.; Pathak, S.; von Eschenbach, A. C.; Logothetis, C. J. *Clin. Cancer Res.* **1997**, 2493; (b) Zhao, X. Y.; Malloy, P. J.; Krishan, A. V.; Swami, S.; Navone, N. M.; Peehl, D. M.; Feldman, D. *Nat. Med.* **2000**, *6*, 703.
9. Molecular modeling was performed using ICM software (Molsoft LLC, San Diego, CA), Molsoft (1998) ICM 2.7 Program Manual (Molsoft, San Diego, CA).

10. Molecular modeling was performed using ICM software (Molsoft LLC, San Diego, CA). The docking of the ligands into WT AR LBD was carried out using the ICM docking procedure which is a two step process. Initial docking of ligands were carried out using grid potential representation of the receptor and flexible ligand. Five grid potentials describe the shape, hydrophobicity, electrostatic and hydrogen-bonding potential of the receptor. The conformations from the grid were then optimized with a full atom representation of the receptor and flexible ligand, by an ICM stochastic global optimization algorithm as implemented in version 2.7 of the Molsoft ICM program (references a & b). Molsoft (1998) ICM 2.7 Program Manual (Molsoft, San Diego, CA); (b) Totrov, M.; Abagyan, R. *Proteins Suppl.* **1997**, *1*, 215–220.
11. Synthesis of compound **9**: (3aα,4β,8β,8aα)-4,5,6,7,8,8a-hexahydro-4,8-etheno-1*H*-cyclohepta[*c*]furan-1,3(3a*H*)-dione was made in accordance with the procedure described in Kohler, E. P.; Tishler, M.; Potter, H.; Thompson, H. T. *J. Am. Chem. Soc.* **1939**, *61*, 1057. A solution of the anhydride (1 g, 5.20 mmol) and 10% Pd/C (~20 mg) in EtOAc was shaken under H_2 at 40 psi overnight. The reaction solution was filtered through a pad of Celite eluting with EtOAc and concentrated to give 0.86 g of (3aα,4β,8β,8aα)-4,5,6,7,8,8a-hexahydro-4,8-ethano-1*H*-cyclohepta[*c*]furan-1,3(3a*H*)-dione as a white powder. The anhydride (2.37 g, 12.2 mmol, 1.2 equiv) was combined with 3-trifluoromethylaniline (1.27 mL, 10.2 mmol, 1.0 equiv) in AcOH (45 mL) and heated at 115 °C overnight. After the reaction mixture was cooled to rt, the resulting precipitate was collected, washed with MeOH and dried to give 2.7 g (78.6%) of compound **9** as a white crystalline solid. Compound **8** was synthesized in this fashion using the unsaturated anhydride. Compounds **10** and **11** were synthesized as described above utilizing (3aα,4β,4aα,5aα,6β,6aα)-4,4a,5,5a,6,6a-hexahydro-4,6-etheno-1*H*-cycloprop[*f*]isobenzofuran-1,3(3a*H*)-dione, made as described in Schueler, P. E.; Rhodes, Y. E. *J. Org. Chem.* **1974**, *39*, 2063, as the key intermediate.
12. (a) Compound **12**: 1-(4-bromo-3-methylphenyl)-1*H*-pyrrole-2,5-dione (0.045 g, 0.17 mmol) and *cis*-1,2-dihydrocatechol (0.057 g, 0.51 mmol) were dissolved in toluene (1.0 mL) and heated to 100 °C for 3 days. The crude reaction mixture was purified by preparative silica gel TLC to yield 41 mg (66% yield) of compound **13** as a white solid. Compound **13** was crystallized from 1:1 acetone/hexane to yield crystals adequate for structural determination; (b) Compound **13**: 2-(trimethylsilyloxy)cyclohexadiene (Aldrich) (0.132 mL, 0.703 mmol) and 1-(3,5-dichlorophenyl)-1*H*-pyrrole-2,5-dione (0.234 mmol) were heated in toluene (1.0 mL) at 110 °C for 3 h. MeOH/HCl (4:1) 5 mL was then added and the reaction was stirred at rt for 1 h. The reaction was then diluted with methylene chloride and washed with satd $NaHCO_3$. The organics were then dried over anhydrous Na_2SO_4. The crude material was purified by preparative TLC eluting with 5% EtOAc in methylene chloride to give 0.057 g of compound **13** as a white solid; (c) Compound **14**: 4,5,7,7a-hexahydro-5-methyl-4,7-ethenofuro[3,4-*c*]pyridine-1,3,6(3a*H*)-trione was synthesized as described in Tomisawa, H.; Hongo, H.; Fujita, R.; Kato, H. *Heterocycles* **1977**, *6*, 1765, and reacted with 4-nitronaphthalen-1-amine as described above for compound **8** to yield **14**.